

# Shell-model Hamiltonian from self-consistent mean-field model: $N = Z$ nuclei

Kazunari Kaneko,<sup>a</sup> Takahiro Mizusaki,<sup>b</sup> Yang Sun,<sup>c,d</sup>  
Munetake Hasegawa<sup>d</sup>

<sup>a</sup>*Department of Physics, Kyushu Sangyo University, Fukuoka 813-8503, Japan*

<sup>b</sup>*Institute of Natural Sciences, Senshu University, Tokyo 101-8425, Japan*

<sup>c</sup>*Department of Physics, Shanghai Jiao Tong University, Shanghai 200240, PR China*

<sup>d</sup>*Institute of Modern Physics, Chinese Academy of Sciences, Lanzhou 730000, PR China*

---

## Abstract

We propose a procedure to determine the effective nuclear shell-model Hamiltonian in a truncated space from a self-consistent mean-field model, e.g., the Skyrme model. The parameters of pairing plus quadrupole-quadrupole interaction with monopole force are obtained so that the potential energy surface of the Skyrme Hartree-Fock + BCS calculation is reproduced. We test our method for  $N = Z$  nuclei in the *fpg*- and *sd*-shell regions. It is shown that the calculated energy spectra with these parameters are in a good agreement with experimental data, in which the importance of the monopole interaction is discussed. This method may represent a practical way of defining the Hamiltonian for general shell-model calculations.

*Key words:* Nuclear shell model, Skyrme Hartree-Fock,  $N = Z$  nuclei

*PACS:* 21.60.Cs, 21.60.Jz, 21.60.-n, 21.10.-k

---

Nuclear structure study is usually carried out with two major groups of microscopic approaches: the self-consistent mean-field (SCMF) method [1] and the shell model (SM) method [2]. Both approaches have their advantages and disadvantages. The SCMF method has a wide applicability across the nuclear chart for global properties of the ground state, such as the binding energy, nuclear size, and surface deformation. However, it does not give detailed spectra of excited states and wave functions. Beyond mean-field approximations, the angular momentum and particle number projection method has been applied; but it has been pointed out that there are some conceptual problems and numerical difficulties [3,4]. On the other hand, the SM method has the advantage that excited energy levels and wave functions are described properly

with many-body correlations included. However, in the SM approach, the shell model Hamiltonian is required to accord with each truncated model space, and single-particle energies and interaction matrix elements must be specific to the mass region. It is not very clear how to determine these quantities microscopically. There have been attempts along this line by Brown and Richter [5] and by Alhassid, Bertsch, and collaborators [6,7]. In the former attempt, the SCMF was used to determine single-particle energies of the SM Hamiltonian, while in the latter, a procedure for mapping the SCMF onto the SM Hamiltonian, which includes monopole pairing and quadrupole-quadrupole ( $QQ$ ) interactions, was proposed. Very recently, a novel way of determining parameters of the interacting boson model (IBM) Hamiltonian has been proposed by Nomura *et al.* [8] by using the potential energy surfaces (PES's) of the SCMF model.

A realistic SM Hamiltonian can in principle be derived from the free nucleon-nucleon force, and in fact, such microscopic interactions have been proposed for the  $pf$  shell [9,10]. However, they fail to reproduce excitation spectra, binding energies, and transitions if many valence nucleons are involved. To overcome this defect, considerable effort has been put forward on effective interactions with empirical fit to experimental data [11,12,13]. On the other hand, realistic effective interactions in nuclei are expressed in terms of multipole pairing, multipole particle-hole, and monopole interactions, the dominant parts of which are the monopole pairing and quadrupole-quadrupole interactions with monopole terms ( $PQQM$ ) [14]. This has actually been confirmed for a wide range of  $N \approx Z$  nuclei in a series of calculations with an extended  $PQQM$  interactions including additional terms (the quadrupole pairing and the octupole-octupole term) [15,16]. This extended  $PQQM$  model has been successfully applied to different nuclei, as for instance those in the  $fp$ -shell region [15] and the  $fpg$ -shell region [16]. The model has only several parameters, far less than the number of realistic interaction matrix elements usually contained in shell model calculations. However, its capability is very much comparable to that of realistic effective interactions. Thus, the extended  $PQQM$  model is not a mere schematic model, but is a kind of realistic shell model calculation applicable to a large body of nuclei.

In general, defining an effective SM Hamiltonian, especially for heavier nuclei where truncation in the shell model space is necessary, is a very difficult task. It is desired that a SM Hamiltonian is determined at a more fundamental level, which can not only locally fit excitation spectra, but also be consistent with a global description of the ground state properties. It has been claimed [17] that within the SCMF method, the Skyrme force contains correct  $QQ$  and monopole components, and is able to describe both low- and high-energy quadrupole excitations. The Skyrme force including pairing interaction contains  $QQ$  and pairing, as well as monopole components. It is the purpose of the present Letter that based on the Skyrme SCMF, we propose the Hamil-

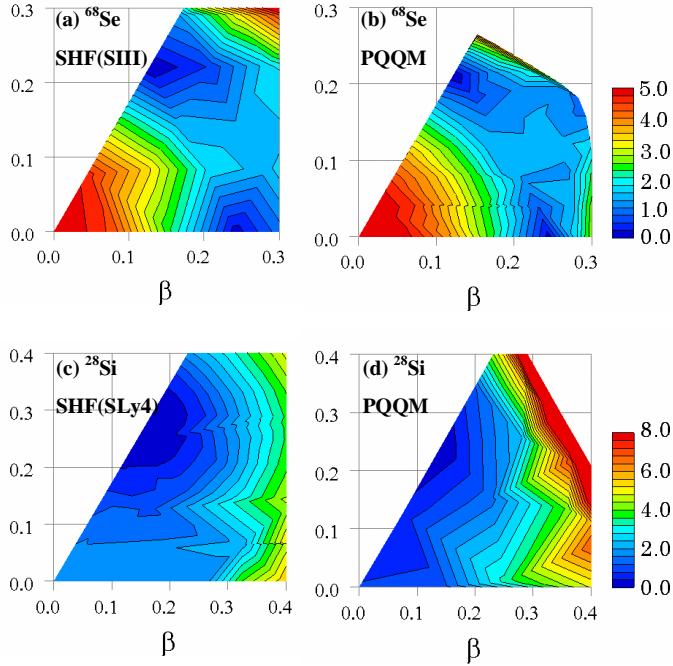


Fig. 1. (Color online) PES's for  $^{68}\text{Se}$  and  $^{28}\text{Si}$  in the SHF calculation (a and c) and the *PQQM* shell-model calculation (b and d). The *PQQM* parameters are determined so that the *PQQM* PES reproduces approximately that of the SHF. Contour spacings are 0.2 MeV and 0.4 MeV for upper and lower graphs, respectively.

tonian for the truncated shell model by performing a global PES mapping. We note that for a shell model using realistic effective interactions, it may be very difficult to obtain a unique result when such a global PES mapping is performed because there are too many interaction matrix elements in the model. However, our *PQQM* model Hamiltonian has only few parameters, namely, the  $g_0$ ,  $\chi$ , and monopole strengths (see Eq. (1) below). Therefore, the *PQQM* type of interaction is particularly suitable for a global PES mapping.

Figure 1a and 1c show PES's on the  $\beta$ - $\gamma$  plane calculated by the constrained Skyrme Hartree-Fock + BCS method (hereafter denoted as SHF), which is imposed by the triaxial degrees of freedom using the mass quadrupole moments. The plotted energy ranges are up to 5 MeV for  $^{68}\text{Se}$  and 8 MeV for  $^{28}\text{Si}$  above the respective energy minimum. For  $^{68}\text{Se}$ , we employ the SIII parameter set [18] of the Skyrme interaction for the mean-field channel, which has been successful in describing systematically the ground-state quadrupole deformations in proton- and neutron-rich Kr, Sr, Zr, and Mo isotopes [19]. For  $^{28}\text{Si}$ , we use the SLy4 [20] interaction. We use the ev8 code [21] with pairing interaction of the  $\delta$ -function type with the strength  $V_0 = 1000 \text{ MeV fm}^3$ . For  $^{68}\text{Se}$ , the long-standing prediction of a stable oblate deformation was confirmed by the observation of the oblate ground state band in  $^{68}\text{Se}$  [22]. Determination of shape was inferred indirectly from the study of rotational bands, while direct quadrupole measurement is difficult for these short-lived

states. It has been suggested by various theoretical approaches [23,24,25,26,27] that the oblate configuration coexists with a prolate rotational band, which constitutes a clear example of oblate-prolate shape coexistence. It can be seen from Fig. 1 that the PES of the current SCMF calculation with SIII interaction (Fig. 1a) indeed yields two separate minima at the oblate and prolate side with deformation  $\beta \approx 0.24$ . For  $^{28}\text{Si}$ , the PES (Fig. 1c) has a minimum at the oblate side with deformation  $\beta \approx 0.33$ , corresponding to the experimental spectroscopic quadrupole moment  $Q_s = 16 \text{ efm}^2$ .

To connect these SHF results with SM results, we start with the *PQQM* model Hamiltonian [27,28]

$$H = \sum_{\alpha} \varepsilon_{\alpha} c_{\alpha}^{\dagger} c_{\alpha} - \frac{g_0}{2} P_0^{\dagger} \cdot P_0 - \frac{\chi}{2} Q_2^{\dagger} \cdot Q_2 + V_{\text{m}}, \quad (1)$$

where  $\varepsilon_{\alpha}$  is single-particle energy. The second term in Eq. (1) is the monopole pairing interactions with  $P_0$  being the  $T = 1$ ,  $J = 0$  pair operator, and the third term is the  $QQ$  interaction with  $Q_2$  the  $T = 0$  quadrupole operator. The last term  $V_{\text{m}}$  is the monopole force. Due to isospin-invariance, each of these terms in Eq. (1) contains the  $p$ - $n$  components which play important roles in  $N = Z$  nuclei. The quadrupole-pairing, the octupole-octupole, and the average monopole terms employed in the previous papers [27,28] are neglected for simplicity because they do not affect the current conclusion.

The SM calculation [27,28] is performed by the SM code [29] for the *fpg*- and *sd*-SM spaces, for which we assume a closed  $^{56}\text{Ni}$ - and  $^{16}\text{O}$ -core, respectively. Since the Hamiltonian (1) is isospin-invariant, single-particle energies are taken as the same for protons and neutrons. For the *fpg*-shell space, the single-particle energies for the  $2p_{3/2}$ ,  $1f_{5/2}$ ,  $2p_{1/2}$ , and  $1g_{9/2}$  states can be read from the low-lying states of  $^{57}\text{Ni}$ . We use the experimental values  $\varepsilon_{p3/2} = 0.0$ ,  $\varepsilon_{f5/2} = 0.77$ ,  $\varepsilon_{p1/2} = 1.11$ , and  $\varepsilon_{g9/2} = 2.50$  (all in MeV), as in the previous paper [27]. For the *sd*-shell space, the single-particle energies for the  $1d_{5/2}$ ,  $2s_{1/2}$ , and  $1d_{3/2}$  states are employed from USD Hamiltonian [11]. Nuclear shapes including triaxiality are calculated by the constrained Hartree-Fock (CHF) method [30,31] and SM PES is defined as the expectation value  $\langle H \rangle$  with respect to the CHF state in the  $\beta$ - $\gamma$  plane.

We now sketch the procedure to determine the pairing, the quadrupole-quadrupole, and the monopole force strengths by taking  $^{68}\text{Se}$  and  $^{28}\text{Si}$  as examples. Figure 2 shows the PES's as functions of axial deformation  $\beta$  and of triaxiality  $\gamma$  with fixed  $\beta$  at the deformation minimum. The PES results in solid curves are obtained by requiring that the interaction strengths in the *PQQM* Hamiltonian are set so as to reproduce the PES's of the SHF calculation. As one can see, the PES's of the *PQQM* calculation reproduce well those of the SHF with SIII for  $^{68}\text{Se}$  and SLy4 for  $^{28}\text{Si}$ . For large deformations with  $|\beta| > 0.24$

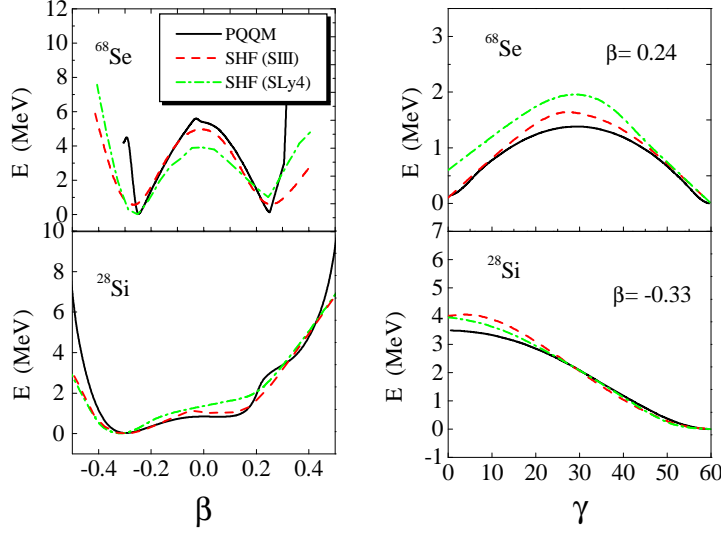


Fig. 2. (Color online) PES's for axial and fixed  $\beta$  deformations in  $^{68}\text{Se}$  and  $^{28}\text{Si}$ . The left and right panels show PES's along axial oblate-to-prolate  $\beta$  deformation and variation with triaxiality with fixed  $\beta$  at the minimum.

in  $^{68}\text{Se}$  and  $|\beta| > 0.4$  in  $^{28}\text{Si}$ , the PES's have the pronounced sharp wall as shown in Fig. 2. This seems to be a general trend and is probably due to the small truncated model space. We therefore neglect this sharp wall in the PES mapping. In this way, the *PQQM* parameters are uniquely determined.

It is known that the SHF PES pattern depends on the Skyrme parameterization. To show that the extracted *PQQM* Hamiltonian has a general meaning, we present in Fig. 2 also the results for each nucleus with one more Skyrme interaction, namely the PES's of SHF with SLy4 for  $^{68}\text{Se}$  and SIII for  $^{28}\text{Si}$ . Comparing the results, we see that the curves depend only weakly on the choice of the Skyrme interaction. The essential PES pattern such as shape coexistence of  $^{68}\text{Se}$  does not alter with a particular parametrization. This fact has also been realized by the earlier paper [8]. Here we confirm it for  $^{28}\text{Si}$  and  $^{68}\text{Se}$  using different Skyrme interactions. For  $^{28}\text{Si}$ , the interaction strengths in the *PQQM* Hamiltonian obtained from the Skyrme interaction SIII are almost the same as those from SLy4. For  $^{68}\text{Se}$ , the quadrupole interaction has to be modified in order to fit the SHF-SLy4 PES pattern; however it is only a small reduction when comparing it with the quadrupole interaction extracted from the SHF-SIII PES pattern.

The so-obtained *PQQM* force strengths for the *fpg*-shell space are  $g_0 = 0.270(64/A)$  and  $\chi = 0.222(64/A)^{5/3}/b^4$ , with  $b$  the length of harmonic oscillator, and the  $T = 1$  monopole force strength is  $V_m(f_{5/2}, p_{1/2}; T = 1) = -0.25$  MeV. The *PQQM* Hamiltonian determined in this way describes quite well the global properties of these nuclei. In particular, the effect of the monopole shift is found to be important for producing the oblate minimum. We note that in the previous paper [27], the deformation  $\beta = 0.20$  from the SM cal-

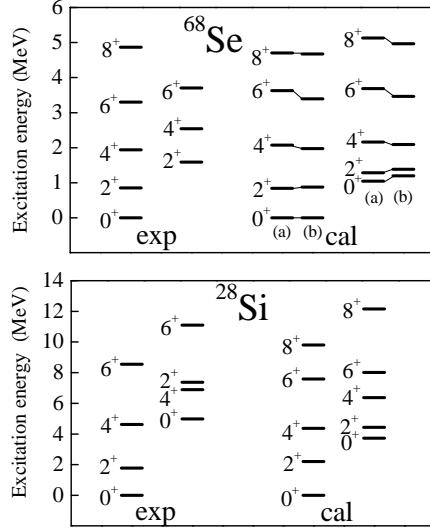


Fig. 3. Comparison between experimental and calculated energy levels for  $^{68}\text{Se}$  and  $^{28}\text{Si}$  with the  $PQQM$  interactions determined in the present Letter. In the upper graph for  $^{68}\text{Se}$ , the calculated energy levels with the  $PQQM$  parameters obtained from SIII (marked as (a)) and SLy4 PES's (marked as (b)) are shown for the ground-state and side bands.

calculation with effective charges  $e_\pi = 1.5e$  and  $e_\nu = 0.5e$  was smaller than  $\beta = 0.24$  estimated from the experimental quadrupole moment. Larger effective charges  $e_\pi = 1.75e$  and  $e_\nu = 0.75e$  were therefore needed to obtain the oblate minimum with  $\beta = 0.24$ . Now our new result for  $^{68}\text{Se}$  with the SM PES calculated from the  $PQQM$  Hamiltonian shows correctly the coexistence of the prolate and oblate minimum at  $|\beta| \approx 0.24$  (see Fig. 1b).

It should be noted that the PES of the standard IBM-2 may not properly describe triaxial deformation and coexistence of oblate and prolate shapes because there is no stabilized triaxiality in its mean field solution, which can be seen from the expectation value of the IBM Hamiltonian in Eq. (3) of Ref. [8].

The  $PQQM$  PES for the  $N = Z$  nucleus  $^{28}\text{Si}$  is shown in Fig. 1d, which is compared to the SHF results with the SLy4 interaction in Fig. 1c. The interaction strengths thus-obtained are  $g_0 = 0.50$  and  $\chi = 4.158A^{-2/3}/b^4$ , with the monopole interaction strengths  $V_m(d_{5/2}, d_{3/2}; T = 1) = -0.20$  and  $V_m(s_{1/2}, s_{1/2}; T = 1) = 1.0$  MeV. In Fig. 2, the PES's along the axial deformation and as a function of triaxiality with fixed minimum  $\beta$  are shown. The SM calculation with effective charges  $e_\pi = 1.5e$  and  $e_\nu = 0.5e$  yields a deformation  $\beta = -0.33$  as in the SLy4 PES (see Fig. 2).

In Fig. 3, we compare energy levels between experiment and our SM calculation for  $^{68}\text{Se}$  and  $^{28}\text{Si}$ , obtained with the  $PQQM$  interaction strengths determined from the above procedure. For  $^{68}\text{Se}$ , we show energy spectra obtained

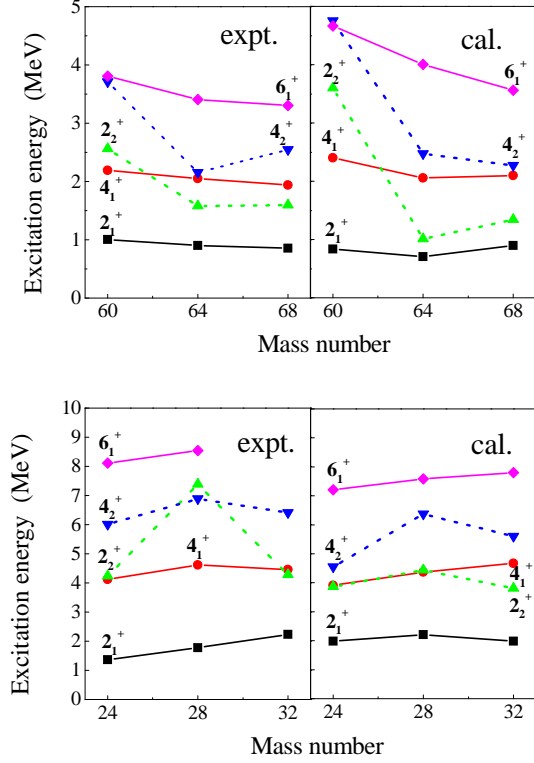


Fig. 4. (Color online) Calculated energy levels compared with data for the  $N = Z$  nuclei in the sd- and fpg-shell regions. The upper and lower panels represent results for  $^{60}\text{Zn}$ ,  $^{64}\text{Ge}$ ,  $^{68}\text{Se}$ , and for  $^{24}\text{Mg}$ ,  $^{28}\text{Si}$ ,  $^{32}\text{S}$ , respectively.

with different PQQM parameters which are determined from the PES's using the Skyrme interactions SIII and Sly4. It is seen that the two calculated energy spectra are resemble each other. Both the experimental ground and side bands for  $^{68}\text{Se}$  are nicely reproduced. This indicates that the PQQM Hamiltonian derived from a good PES of the SHF method works well for producing detailed energy spectra. In Ref. [27], the previous *fpg*-SM calculation for  $^{68}\text{Se}$  using the phenomenologically-fitted force strengths achieved a reasonable agreement with data. We note that the *PQQM* force strengths proposed in this Letter are close to those fitted ones in [27]. The calculation for  $^{68}\text{Se}$  predicts the first excited  $0_2^+$  state. Our analysis for quadrupole moments indicates that the ground-state has an oblate deformation and the side band has a prolate shape. For  $^{28}\text{Si}$ , the calculated ground band reproduces the data well. The calculation indicates the side band built on the first excited  $0_2^+$  state; however it does not exhibit the inversion of the second  $2_2^+$  and  $4_2^+$  states as suggested by the current data.

Next we test this procedure with the neighboring  $N = Z$  nuclei of  $^{68}\text{Se}$  and  $^{28}\text{Si}$ . Figure 4 shows a comparison of our calculated energy levels with data for  $^{60}\text{Zn}$ ,  $^{64}\text{Ge}$ , and  $^{68}\text{Se}$ , and for  $^{24}\text{Mg}$ ,  $^{28}\text{Si}$ , and  $^{32}\text{S}$ . The calculation correctly reproduces the trend of level variation as mass number changes, with only one exception in the second excited  $2_2^+$  state of  $^{28}\text{Si}$ , as mentioned before.

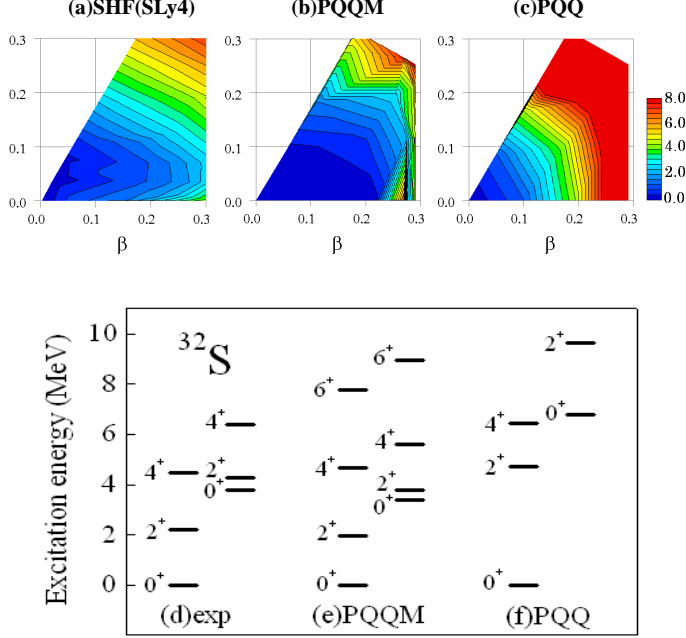


Fig. 5. (Color online) PES's and energy levels for  $^{32}\text{S}$ . (a) PES of the SHF(SLy4), (b) PES of the  $PQQM$  model, (c) PES of the  $PQQ$  model (without monopole interactions). In the lower plot, the SM energy levels of  $PQQM$  in (e) and  $PQQ$  in (f) are compared with experimental data in (d). Contour spacings in a, b and c are 0.4 MeV.

$E2$  transition probabilities for the positive-parity yrast and excited states in  $^{28}\text{Si}$  and  $^{68}\text{Se}$  are shown in Table I. For  $^{28}\text{Si}$ , our calculated  $B(E2)$  values are in good agreement with the experimental data. For  $^{68}\text{Se}$ , the quadrupole deformation obtained from our calculated  $B(E2; 2_1^+ \rightarrow 0_1^+)$  is  $\beta \sim 0.26$ , which is consistent with the experimental estimation  $\beta \sim 0.27$  by Fischer *et al.* [22] and 0.30 by Jenkins *et al.* [32]. In Table I, we list also the theoretical  $B(E2)$  values by Petrovici *et al.* [24] with the Excited Vampir calculation. Their estimated deformation is  $\beta \sim 0.37$ , which is much larger than ours, and inconsistent with the experimental estimation.

We take  $^{32}\text{S}$  as an example to discuss the monopole effects on PES. The monopole interaction  $V_m(d_{5/2}, d_{3/2}; T = 1)$  between the spin-orbit partners  $d_{5/2}$  and  $d_{3/2}$  is known to be very important for the  $sd$ -shell spectra. As the Fermi energy approaches the  $d_{3/2}$  orbit, the monopole interactions  $V_m(d_{5/2}, d_{3/2}; T = 1)$  and  $V_m(s_{1/2}, s_{1/2}; T = 1)$  act on the relevant orbits and affect both PES and energy levels. In Fig. 5, the PES's and energy levels in the SM calculation with and without the monopole force are respectively compared with the SHF PES's and with experimental energy levels. The energy range is up to 8 MeV above the energy minimum. Figure 5b exhibits PES's of the  $PQQM$  model calculated with the determined parameters by comparison with the PES's of the SLy4 interaction in Fig. 5a. The calculated energy levels are shown in



Table 1

Calculated  $B(E2)$  values for positive-parity yrast and excited states in  $^{28}\text{Si}$  and  $^{68}\text{Se}$ , which are compared with the known experimental ones for  $^{28}\text{Si}$  and the theoretical values of Petrovici *et al.* [24] for  $^{68}\text{Se}$ , respectively.

	$^{28}\text{Si}$ [ $e^2\text{fm}^4$ ]		$^{68}\text{Se}$ [ $e^2\text{fm}^4$ ]	
$I_i^\pi \rightarrow I_f^\pi$	Expt.	Calc.	Petrovici <i>et al.</i>	Calc.
$2_1^+ \rightarrow 0_1^+$	66.7	55.7	966	503.3
$4_1^+ \rightarrow 2_1^+$	69.7	51.2	1381	609.6
$6_1^+ \rightarrow 4_1^+$	50.0	54.5	1402	594.6
$8_1^+ \rightarrow 6_1^+$		34.9	1710	
$0_2^+ \rightarrow 2_1^+$	43.4	99.7		
$2_2^+ \rightarrow 0_2^+$				511.7
$4_2^+ \rightarrow 2_2^+$				553.8
$6_2^+ \rightarrow 4_2^+$				495.4
$8_2^+ \rightarrow 6_2^+$				44.1

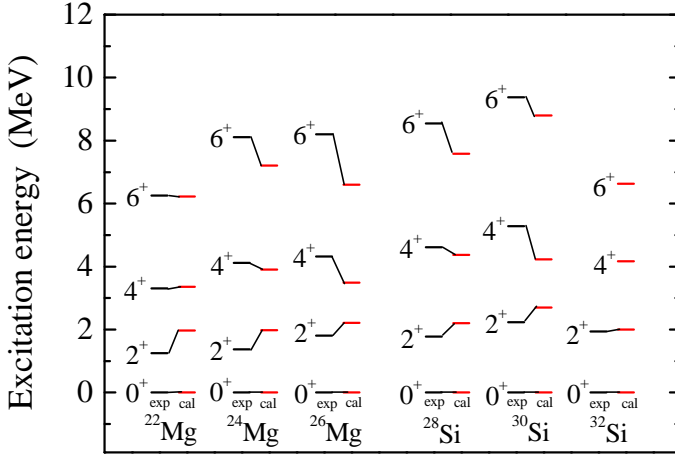


Fig. 6. (Color online) Calculated energy levels compared with experimental data for the Mg and Si isotopic chains.

Fig. 5e, which are compared with data in Fig. 5d. As can be seen, the  $PQQM$  calculation with the present interaction strengths reproduces data well. To see the monopole effects on PES and energy levels, we switch off all the monopole interactions and show the results in Fig. 5c and 5f. One sees that the PES in Fig. 5c does not reproduce that of Fig. 5a, and the calculated energy levels in Fig. 5f lie too high when compared with data. We thus conclude that the monopole force  $V_m$  is important for a correct reproduction of both the SHF PES and experimental energy levels in  $^{32}\text{S}$ .

Finally, we show in Fig. 6 a systematical comparison between theory and

experiment for the energy levels along the Mg and Si isotopic chains. We can see that the calculated energy levels for the low-lying  $2^+$  and  $4^+$  states reproduce fairly well those of the experimental data, while the  $6^+$  states lie a little higher than experiment.

To summarize, for a correct SM description of nuclear spectra phenomenologically-adjusted effective interactions are usually introduced. In the present Letter, we have presented a procedure to define the SM Hamiltonian for a truncated space at a more fundamental level, by performing a global PES mapping with the SCMF results of the Skyrme interaction. The parameters of the *PQQM* model have been determined so as to reproduce the overall pattern of the PES of the SHF calculation. The *PQQM* SM calculations with the determined forces have reproduced well the experimental energy levels for the  $N = Z$  nuclei in the *fpg*- and *sd*-shell regions. Effects brought by the monopole interactions have been discussed. This work may represent a practical method of defining SM Hamiltonian from microscopic mean-field theories, and therefore may have general applications in other shell models. For example, the Projected Shell Model [33] that employs the separable forces can adopt this method.

In the present work, single-particle energies in the SM calculation are taken from experiment as usual. For consistency, we should have used single-particle energies of the SCMF. However, it is well known that the SHF single-particle energies cannot be directly compared with experimental data. A recent study [34] suggests that fitting the spin-orbit and tensor parts of the SCMF to the spin-orbit splittings improves considerably the single-particle properties of the SCMF. Therefore, there are two possibilities for our choice of single-particle states. One is to use the experimental single-particle energies as in the present work, and the other is to use the improved SCMF single-particle energies that include the tensor interaction. The latter deserves more investigation, and will be our future goal of study. Application of the present method to neutron-rich nuclei including the tensor interaction in the SHF is also in progress.

YS was supported by the National Natural Science Foundation of China under contract 10875077 and by the Chinese Major State Basic Research Development Program through grant 2007CB815005.

## References

- [1] M. Bender, P.-H. Heenen, and P. G. Reinhard, *Rev. Mod. Phys.* **75** (2003) 121.
- [2] B. A. Brwon and G. H. Wildenthal, *Ann. Rev. Nucl. Part. Sci.* **38** (1988) 29.
- [3] J. Dobaczewski, *et al.*, *Phys. Rev. C* **76** (2007) 054315; *Phys. Rev. Lett.* **60** (1988) 2254.

- [4] M. Bender and P.-H. Heenen, Phys. Rev. C **78** (2008) 024309.
- [5] B. A. Brown and W. A. Richter, Phys. Rev. C **58** (1998) 2099.
- [6] Y. Alhassid, G. F. Bertsch, L. Fang, and B. Sabbey, Phys. Rev. C **74** (2006) 034301.
- [7] R. Rodriguez-Guzman, Y. Alhassid, G. F. Bertsch, Phys. Rev. C **77** (2008) 064308.
- [8] K. Nomura, N. Shimizu, and T. Otsuka, Phys. Rev. Lett. **101** (2008) 142501.
- [9] T. T. S. Kuo and G. E. Brown, Nucl. Phys. A **114** (1968) 241.
- [10] M. Hjorth-Jensen, T. T. S. Kuo, and E. Osnes, Phys. Rep. **261** (1995) 125.
- [11] B. A. Brown and B. H. Wildenthal, Ann. Rev. Nucl. Part. Sci. **38** (1988) 29.
- [12] A. Poves and A. P. Zuker, Phys. Rep. **70** (1981) 235.
- [13] M. Honma, T. Otsuka, B. A. Brown, and T. Mizusaki, Phys. Rev. C **69** (2004) 034335.
- [14] M. Dufour and A. P. Zuker, Phys. Rev. C **54** (1996) 1641.
- [15] M. Hasegawa, K. Kaneko, and S. Tazaki, Nucl. Phys. **A688** (2001) 765.
- [16] K. Kaneko, M. Hasegawa, and T. Mizusaki, Phys. Rev. C **66** (2002) 051306(R).
- [17] J. Dobaczewski, W. Nazarewicz, J. Skalski, and T. Werner, Phys. Rev. Lett. **60** (1988) 2254.
- [18] M. Beiner, H. Flocard, N. Van Giai, P. Quentin, Nucl. Phys. **A238** (1975) 29.
- [19] P. Bonche, H. Flocard, P. -H. Heenen, S. J. Krieger, M. S. Weiss, Nucl. Phys. A **443** (1985) 39.
- [20] E. Chabanat *et al.*, Nucl. Phys. **A635** (1998) 231.
- [21] P. Bonche *et al.*, Comput. Phys. Commun. **171** (2005) 49.
- [22] S. M. Fischer *et al.*, Phys. Rev. Lett. **84** (2000) 4064.
- [23] M. Yamagami, K. Matsuyanagi, and M. Matsuo, Nucl. Phys. **A693** (2001) 579.
- [24] A. Petrovici, K. W. Schmid, and A. Faessler, Nucl. Phys. **A710** (2002) 246.
- [25] M. Kobayashi, T. Nakatsukasa, M. Matsuo, and K. Matsuyanagi, Prog. Theor. Phys. **110** (2003) 65.
- [26] Y. Sun, M. Wiescher, A. Aprahamian, J. Fisker, Nucl. Phys. **A758** (2005) 765.
- [27] K. Kaneko, M. Hasegawa and T. Mizusaki, Phys. Rev. C **70** (2004) 051301(R).
- [28] M. Hasegawa, K. Kaneko, T. Mizusaki, and S. Tazaki, Phys. Rev. C **69** (2004) 034324.

- [29] T. Mizusaki, RIKEN Accel. Prog. Rep. **33** (2000) 14.
- [30] T. Mizusaki *et al.*, Phys. Rev. C **59** (1999) R1846.
- [31] K. Hara, Y. Sun, and T. Mizusaki, Phys. Rev. Lett. **83** (1999) 1922.
- [32] D. G. Jenkins *et al.*, Phys. Rev. C **64** (2001) 064311.
- [33] K. Hara and Y. Sun, Int. J. Mod. Phys. E **4** (1995) 637.
- [34] M. Zalewski *et al.*, Phys. Rev. C **77** (2008) 024316.